DOI: 10.19884/j.1672-5220.202405016

Effect of Heat Treatment on Molecular Mass and Thermal Properties of Thermotropic Liquid Crystal Polyesters

DONG Shihang[1], CHEN Yufeng[1], WAN Hai[1], LIANG Yuan[2], HUANG Shuohan[1], WANG Yanping[1], XIA Yumin[1*]

1. Key Laboratory of High Performance Fibers & Products, Ministry of Education, College of Materials Science and Engineering, Donghua University, Shanghai 201620, China
2. College of Physics, Donghua University, Shanghai 201620, China

Abstract: The thermotropic liquid crystal polyester (TLCP) fiber is an increasingly important strategic high-performance fiber. In this paper, the TLCP was prepared by two-step melt polymerization using 4-hydroxybenzoic acid (HBA) and 6-hydroxy-2-naphthoic acid (HNA) as comonomers at a molar ratio of 7∶3. The structure of TLCP was confirmed by the Fourier transform infrared (FTIR) spectrometer and nuclear magnetic resonance (NMR) spectrometer. The thermal and rheological properties of TLCP before and after heat treatment were analyzed systematically by the differential scanning calorimeter (DSC), dynamic mechanical analyzer (DMA) and high-temperature rotational rheometer. The results revealed that the melting temperature, glass transition temperature and melt viscosity of the TLCP increased significantly after heat treatment. It indicates that the crystallization of the TLCP is perfect, and solid-phase condensation occurs during heat treatment, which increases its molecular mass. In conclusion, heat treatment at a temperature below but close to the melting temperature can effectively regulate the structure and properties of the TLCP, and the results of this study can provide a reference for the high strengthening of TLCP fibers.

Keywords: thermotropic liquid crystal polyester (TLCP); heat treatment; viscosity; thermal property

CLC number: TG15; TQ323.4 **Document code**: A

Article ID: 1672-5220(2025)02-0124-12

Open Science Identity (OSID)

0 Introduction

Thermotropic liquid crystalline polyesters (TLCPs) have attracted significant research and commercial attention due to their outstanding thermal stability, mechanical strength and chemical resistance, and low linear thermal expansion coefficient[1-9]. However, their molecular structure, which lacks flexible segments and exhibits a rigid rod-like configuration, leads to strong intermolecular forces, increasing brittle fractures or fatigue cracks. Furthermore, these polyesters have high melting temperatures, posing challenges for processing and limiting their applications[10-12]. To overcome these challenges, several methods have been explored to lower the melting temperature of TLCPs, aiming to strike a balance between the performance and processing temperature. These methods include introducing substituents and flexible groups to mesogenic units, as well as incorporating nonlinear monomers into the molecular chains. For example, poly (hydroxybenzoic acid) (P-HBA), synthesized from a rigid main chain represented by 4-hydroxybenzoic acid (HBA), exhibits an extremely high melting temperature and undergoes decomposition before melting. Conversely, 6-hydroxy-2-naphthoic acid (HNA), a nonlinear monomer with a kinked structure resembling a naphthalene ring, can be copolymerized with HBA to lower the melting temperature and prevent chain stacking[13-24]. By employing these methods, it becomes possible to achieve a balance between the performance and processing temperature in TLCPs, thereby expanding their potential applications.

Melt polymerization is a method of polymerizing monomers at high temperatures, where the polymerization reaction occurs above the melting temperature of both the monomer and the polymer. This process offers advantages such as the reduced energy consumption, the shortened processing time and the improved production efficiency. However, it requires precise control over the ratio and extent of functional groups among monomers. Due to the challenge of precisely controlling the quantity of monomers during polymerization, polydisperse polymers with a wide molecular mass distribution are often produced. Heat treatment can be utilized to enhance the crystallinity and orientation of polymers, thereby improving their performance[25-29]. Reyes et al.[30] reported that molecular rearrangement during heat treatment could effectively adjust the physical properties of TLCPs by controlling their microstructure. The results

Received date: 2024-05-27

Foundation item: National Key Research and Development Program of China (No. 2021YFB3700105)

* Correspondence should be addressed to XIA Yumin, email: xym@dhu.edu.cn

Citation: DONG S H, CHEN Y F, WAN H, et al. Effect of heat treatment on molecular mass and thermal properties of thermotropic liquid crystal polyesters[J]. *Journal of Donghua University (English Edition)*, 2025, 42(2): 124-135.

indicate an increase in the melting temperature, crystallinity and tensile modulus of TLCPs. These findings provide valuable insights for further optimizing the performance and processing of TLCPs.

This study utilized a two-step melt polymerization method to prepare the TLCP at a molar ratio of HBA to HNA of 7∶3 (denoted as B70-N30). Firstly, the structures of the monomers before and after acetylation and the synthesized TLCP were compared using the Fourier transform infrared (FTIR) spectrometer, nuclear magnetic resonance (NMR) spectrometer and differential scanning calorimeter (DSC). Secondly, solid-phase condensation was conducted on the TLCP at different heat treatment temperatures of 240, 250 and 260 ℃, and at different heat treatment times of 2, 4, 6, 8 and 10 h. Finally, the effects of the heat treatment temperature and time on the melting temperature, glass transition temperature and molecular mass of the TLCP were analyzed using the DSC, dynamic mechanical analyzer (DMA) and high-temperature rotational rheometer.

1 Materials and Methods

1.1 Materials

HBA and HNA were supplied by Zhejiang Shengxiao Chemical Company (Quzhou, China). Acetic anhydride was purchased from Shanghai Titan Technology Company (Shanghai, China).

1.2 Preparation

The TLCP at a molar ratio of 7∶3 of HBA to HNA was prepared by a two-step melt polymerization method, as shown in Fig. 1. In the acetylation reaction step, HBA and HNA were separately added to a round-bottom flask equipped with a mechanical stirrer and a condenser. An excess amount of acetic anhydride was added for the acetylation of monomers having hydroxyl groups. The acetylation was carried out at 150 ℃ for 3 h, after which the acetylated monomers, 4-acetoxy-benzoic acid (ABA) and 6-acetoxy-2-naphthalic acid (ANA), were rapidly cooled in a water bath and fully dried in a vacuum oven. The acetylated monomers and catalyst were added together into a three-neck round-bottom flask equipped with a mechanical stirrer, an N_2 inlet and a condenser. The reaction was performed under a constant flow of N_2. The process commenced with a gradual linear heating of the mixture from 260 ℃ to 280 ℃, where it underwent reaction for 3.0 h. Subsequently, the temperature was incrementally raised to 300 ℃ and sustained for 1.5 h. Following this phase, the temperature was further elevated to 320 ℃ at which the reaction was maintained for an additional 1.5 h. Finally, to ensure thorough polymerization, the reaction mixture was subjected to a vacuum environment for 0.5 h. To characterize the structure, thermal and mechanical properties, the TLCP was injection molded into three different shapes of specimens: dumbbell-shaped (75 mm × 12.5 mm × 2.0 mm, with a narrow section in the middle measuring 25 mm × 4 mm × 2.0 mm), rectangular (50 mm × 7 mm × 2.0 mm), and cylindrical (*Φ*25 mm × 2.0 mm, where *Φ* represents the diameter). For solid-phase condensation, the TLCP powder and injection molded samples were subjected to heat treatment at different temperatures (240, 250 and 260 ℃) and times (2, 4, 6, 8 and 10 h) using a DSC.

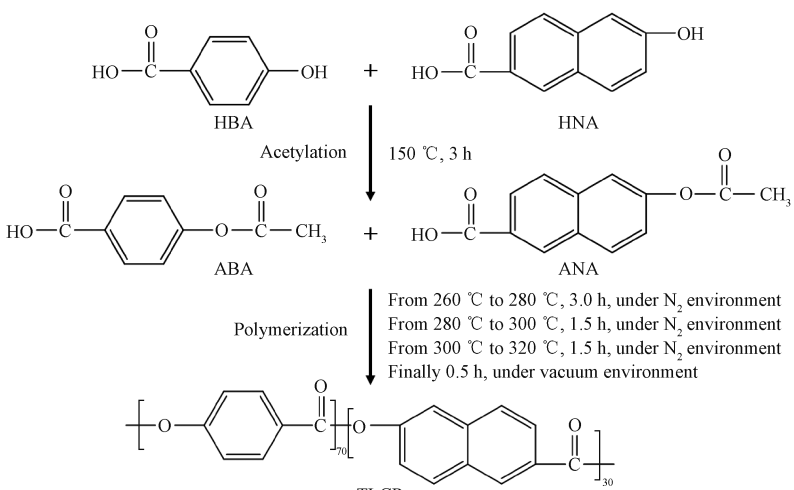

Fig. 1 Reaction route of TLCP

1.3 Characterization

The monomers were analyzed by using an FTIR spectrometer (Nicolet iS10, Thermo Fisher Scientific, Germany) to investigate any changes before and after acetylation. The spectra were acquired in a wavenumber range of 4 000 cm^{-1} to 400 cm^{-1}.

The ^{1}H-NMR spectra of the monomers were obtained using an NMR spectrometer (ADVANCE400, Bruker Corporation, Germany) to analyze their chemical compositions.

The thermal properties of the TLCP were analyzed using a DSC (214 Polyma, NETZSCH-Gerätebau GmbH,

Germany) in a temperature range of 20 ℃ to 350 ℃ under N_2 environment. The heating and cooling rates were set at 20 ℃/min. The monomers were analyzed using a DSC before and after acetylation. The temperature ranges were set at 20–230 ℃ and 20–260 ℃, respectively, with two heating and cooling cycles.

The rectangular samples of the injection-molded TLCP were analyzed using a DMA (DMA8000, PerkinElmer, USA). The samples were heat-treated at temperatures of 240, 250 and 260 ℃ for 2 h, respectively, before testing. The measurement system employed a single cantilever test method in a testing temperature range of −100 ℃ to 200 ℃ at a heating rate of 0.5 ℃/min, a static force of 0.05 N, an elongation of 0.002 mm, a data acquisition interval of 0.5 s, and a frequency of 1 Hz. Liquid nitrogen purging was utilized at a flow rate of 20 mL/min.

The melt rheology of the cylindrical injection-molded TLCP specimens under an oscillatory dynamic shear was analyzed with the aid of a rheometer (MCR702, Anton Paar, Austria) with parallel plate geometry. Dynamic frequency sweep tests were carried out in a frequency range of 0.001 rad/s to 100 rad/s.

2 Results and Discussion

2.1 Analysis of chemical structure

Figure 2 illustrates the ^{1}H-NMR spectra of the monomers before and after acetylation. In the ^{1}H-NMR spectrum of HBA (Fig. 2(a)), the peak at chemical shift of 7.80 corresponds to the hydrogen atom adjacent to the carboxyl group on the benzene ring, while the peak at 6.80 represents the hydrogen atom adjacent to the hydroxyl group on the benzene ring. Additionally, the peak at 10.20 corresponds to the hydrogen atom in the hydroxyl group of HBA, and the peak at 12.40 corresponds to the hydrogen atom in the carboxyl group of HBA. In the ^{1}H-NMR spectrum of HNA (Fig. 2(b)), the peak at 12.80 represents the hydrogen atom in the carboxyl group, while the peaks at 8.46, 7.94 and 7.75 correspond to the hydrogen atoms near the carboxyl group on the naphthalene ring. The peaks at 7.85, 7.18 and 7.15 represent the hydrogen atoms near the hydroxyl group on the naphthalene ring. The peak at 10.13 corresponds to the hydrogen atom on the hydroxyl group of HNA. The ^{1}H-NMR spectra of ABA and ANA reveal that the peaks at position "a" disappear, and the peaks related to the acetyl group emerge at 2.30. This observation confirms that HBA and HNA have been fully acetylated.

Figures 2(c) and 2(d) show the DSC curves for the four monomers: HBA, HNA, ABA and ANA in the first (denoted as HBA-1, HNA-1, ABA-1 and ANA-1, respectively) and second heating cycles (denoted as HBA-2, HNA-2, ABA-2 and ANA-2, respectively). During the second heating cycle, the melting temperatures of ABA and ANA are determined to be 187.4 ℃ and 219.8 ℃, respectively. These values are consistent with the commercially available samples' melting temperatures.

The acetylation process of the monomers was investigated by using the FTIR spectrometer, and the results are presented in Fig. 2 (e). The peak at 3 380 cm^{-1} is associated with the stretching vibration of the O—H in the monomer. The peaks at 1 370 and 1 760 cm^{-1} are attributed to the stretching vibrations of the C—H and C═O within the acetoxy group, respectively. Upon the acetylation of HBA and HNA, the O—H absorption peak vanishes, and two new absorption peaks appear, corresponding to the C═O and C—H in the acetoxy group. These peaks disappear following polymerization. Figure 2(f) reveals an absorption peak at 3 070 cm^{-1}, attributed to the stretching vibration of the C—H on the aromatic ring, and a strong absorption peak at 1 730 cm^{-1}, assigned to the vibration of the C═O in the ester group. As shown in the magnified region from 1 300 cm^{-1} to 1 650 cm^{-1} in Fig. 2(f), the peaks at 1 413, 1 505 and 1 600 cm^{-1} correspond to the stretching vibrations of the C═C on the benzene ring, aligning with the FTIR spectrum of ABA; whereas the peaks at 1 340, 1 470 and 1 630 cm^{-1} are associated with the naphthalene ring structural units, matching the FTIR spectrum of ANA. The presence of these functional group characteristic absorption peaks confirms the successful preparation of the TLCP.

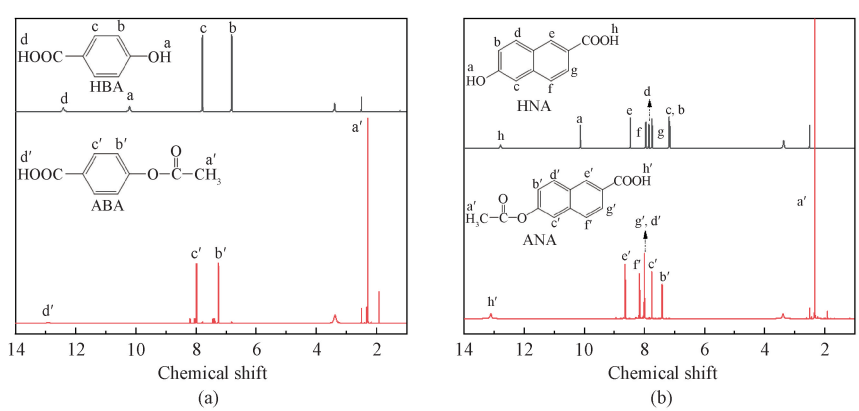

(a) (b)

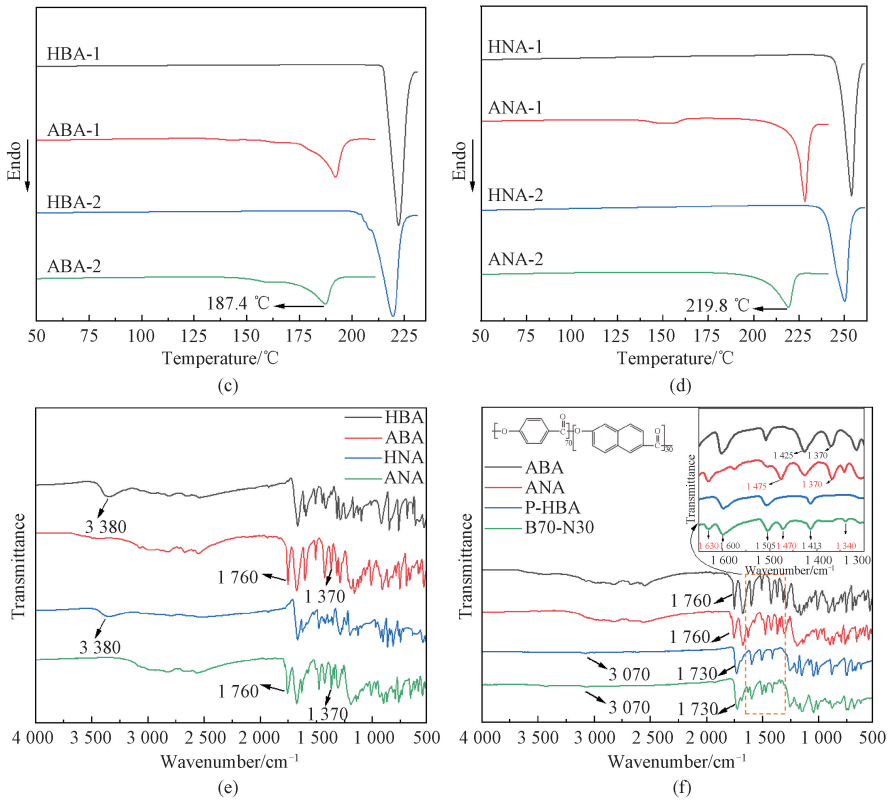

Fig. 2 Chemical structure analysis of monomers and TLCP: (a) ^{1}H-NMR spectra of HBA and ABA; (b) ^{1}H-NMR spectra of HNA and ANA; (c) DSC curves of HBA and ABA during heating; (d) DSC curves of HNA and ANA during heating; (e) FTIR spectra of monomers before and after acetylation; (f) FTIR spectra of TLCP

2.2 Effect of heat treatment on melting and crystallization temperatures

Figure 3 shows the DSC curves of the TLCP during the second heating and cooling cycle, with results summarized in Table 1. The melting temperature T_{m2} and crystallization temperature T_{c2} of the TLCP during the second heating and cooling cycle increase significantly. The crystallization temperature of the TLCP increases from 220.3 ℃ to a maximum of 223.7 ℃. Moreover, the crystallization temperature is positively proportional to the heat treatment time. After heat treatment, the molecular chains of the TLCP align in an orderly manner. This alignment enhances the cohesion and directionality of molecular interactions, thereby forming a more complete crystal structure. The increase in the crystallization temperature is correlated with a higher crystallinity, which enhances its stability and heat resistance in high-temperature environments[31-32]. It can be seen that after eliminating the thermal history, treating the TLCP at 240 ℃ for 8 h increases the melting temperature from 260.9 ℃ to 264.1 ℃. Similarly, treating the TLCP at 250 ℃ for 8 h increases the melting temperature to 264.9 ℃, and treating it at 260 ℃ for 4 h raises the melting temperature to 264.6 ℃. Therefore, it can be concluded that increasing the heat treatment temperature is beneficial to the solid-phase condensation reaction[33-34]. With the increase in the heat treatment temperature, the reactivity of end groups in the amorphous region and the diffusion rate of small molecules increase, promoting solid-phase condensation. However, further extending the treatment time for solid-phase condensation leads to a decrease in the melting temperature of the TLCP. This is due to the occurrence of not only condensation reactions involving end functional groups but also chain exchange reactions in the solid-phase condensation process, resulting in the recombination of chain structural units. On the one hand, the reaction between end functional groups can increase the molecular mass, while chain exchange reactions do not necessarily lead to an increase in the molecular mass and sometimes result in a decrease. On the other hand, the slower diffusion of small molecules due to the adhesive linkage of granular samples leads to an increase in by-products within the granular samples, resulting in a lower melting temperature.

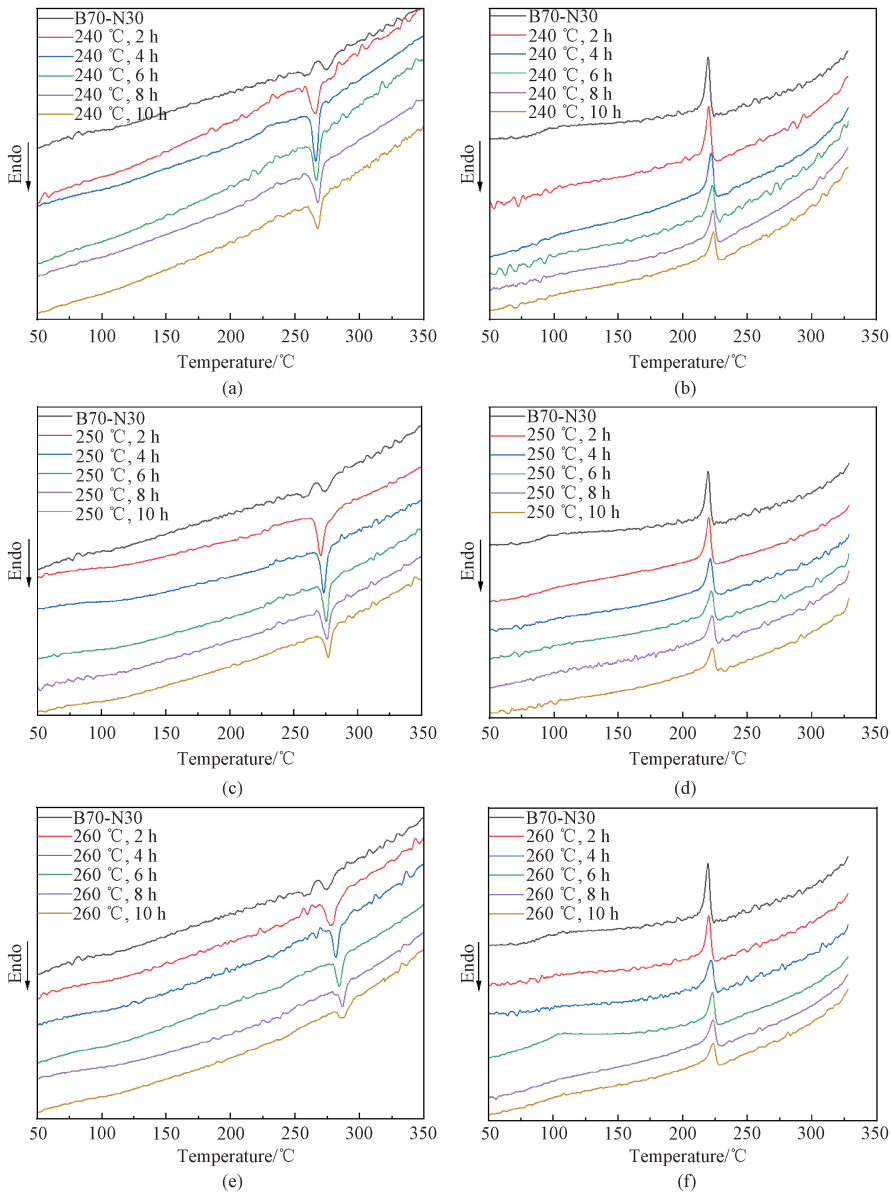

Fig. 3 DSC curves of TLCP: (a) DSC heating curves of TLCP after heat treatment at 240 ℃ for different times; (b) DSC cooling curves of TLCP after heat treatment at 240 ℃ for different times; (c) DSC heating curves of TLCP after heat treatment at 250 ℃ for different times; (d) DSC cooling curves of TLCP after heat treatment at 250 ℃ for different times; (e) DSC heating curves of TLCP after heat treatment at 260 ℃ for different times; (f) DSC cooling curves of TLCP after heat treatment at 260 ℃ for different times

Table 1 Thermal properties of TLCP after heat treatment for different times

Treatment temperature/℃	Treatment time/h	Thermal property	
		T_{c2}/℃	T_{m2}/℃
240	0	220.3	260.9
	2	220.9	261.9
	4	222.4	263.6
	6	223.0	263.7
	8	223.4	264.1
	10	223.5	262.9

(Table 1 continued)

Treatment temperature/℃	Treatment time/h	Thermal property	
		T_{c2}/℃	T_{m2}/℃
250	0	220.3	260.9
	2	220.6	261.7
	4	221.7	263.8
	6	222.2	264.2
	8	223.3	264.9
	10	223.4	263.1
260	0	220.3	260.9
	2	221.0	262.6
	4	222.1	264.6
	6	223.2	264.2
	8	223.6	263.4
	10	223.7	263.3

2.3 Effect of heat treatment on glass transition temperature

The DMA curves of the injection-molded TLCP samples are presented in Fig. 4. The storage modulus exhibits a continuous decrease with the increase of the temperature (E' represents the storage modulus, E'' denotes the loss modulus, and tan δ reflects the material's viscoelastic behavior). The mechanical damping curves, both before and after heat treatment, exhibit three distinct relaxation transitions at approximately −50, 30 and 100 ℃. These transitions are commonly denoted as α, β and γ, from high to low temperatures. The α relaxation process corresponds to the molecular chain movement, which is associated with the glass transition temperature. The β and γ relaxation processes are attributed to multiple transitions resulting from the movement of structural units smaller than the chain segments.

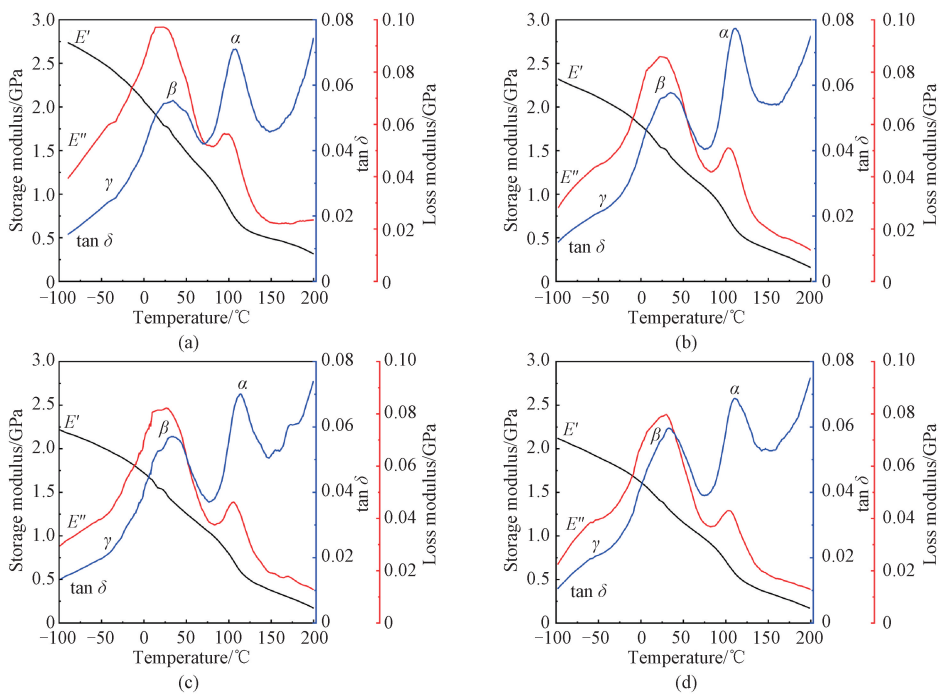

Fig. 4 DMA curves of TLCP: (a) untreated injection parts; (b) injection parts treated at 240 ℃ for 10 h; (c) injection parts treated at 250 ℃ for 10 h; (d) injection parts treated at 260 ℃ for 10 h

Figure 5 presents the relationship between the heat treatment time and tan δ at different temperatures for the TLCP. Table 2 shows the correlation between the relaxation temperatures and the heat treatment time and temperature. It can be observed that after the heat treatment, the α relaxation transition shifts towards higher

temperatures, leading to varying degrees of increased glass transition temperatures[35]. However, there is no direct proportional relationship between the heat treatment time and the glass transition temperature. The maximum value of the glass transition temperature after a heat treatment at 240 ℃ is 110.0 ℃, while it reaches 111.6 ℃ after a heat treatment at 250 ℃, and the maximum value after a heat treatment at 260 ℃ is 110.9 ℃. The experiment results demonstrate that raising the heat treatment temperature enhances the glass transition temperature of the TLCP. However, prolonging the heat treatment time may marginally decrease this temperature. Nonetheless, the glass transition temperature remains higher compared to that of untreated samples. The impact of heat treatment time and temperature on the internal structure of the TLCP is intricate. Appropriate heat treatment facilitates the optimization and organization of the molecular structure of polyesters, concurrently alleviating internal stresses and defects. Extending heat treatment time might increase the molecular mobility and induce reorganization, potentially influencing the glass transition temperature of the TLCP. Additionally, with increasing heat treatment temperature and time, the intensity of the β relaxation process increases, while the intensity of the α relaxation process decreases. Heat treatment above the glass transition temperature of semi-crystalline polymers allows for the movement of the smallest molecular units, leading to the formation of a more perfect crystalline phase. During solid-phase condensation, the TLCP tends to exhibit improved crystallization, and condensation between functional groups further increases the molecular mass. As a result, after heat treatment, the glass transition temperature of the TLCP shifts towards higher temperatures[36].

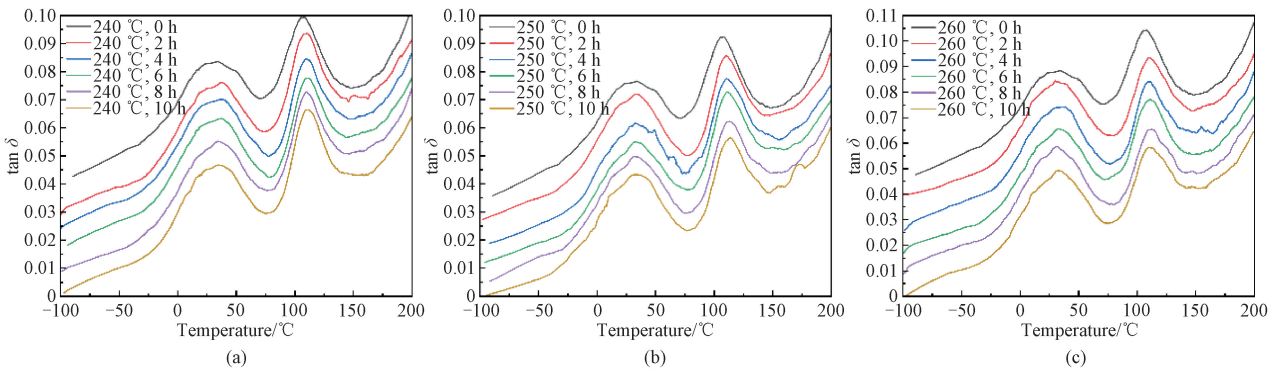

Fig. 5 Evolution of tan δ with heat treatment time at frequency of 1 Hz and different temperatures: (a) 240 ℃; (b) 250 ℃; (c) 260 ℃

Table 2 Correlation between relaxation temperatures and heat treatment time and temperature

Treatment temperature/℃	Treatment time/h	Relaxation temperature/℃	
		β	α
240	0	34.2	108.0
	2	36.3	108.3
	4	35.4	109.8
	6	34.8	110.0
	8	34.3	109.8
	10	34.6	109.4
250	0	34.2	108.0
	2	32.6	110.0
	4	32.6	110.6
	6	31.5	111.0
	8	31.6	110.6
	10	32.3	111.6
260	0	34.2	108.0
	2	30.0	110.0
	4	30.5	109.5
	6	32.8	110.9
	8	31.5	109.2
	10	32.9	109.9

2.4 Effect of heat treatment on molecular mass

TLCPs are a type of anisotropic non-Newtonian fluids. The most significant difference between TLCPs and conventional polymer fluids is the presence of orientational characteristics, which leads to distinct rheological behavior. The viscosity-shear rate flow curve of TLCPs can be divided into three flow regions: region Ⅰ represents the shear-thinning region at low shear rates, where the apparent viscosity decreases rapidly with increasing of the shear rate; region Ⅱ is the quasi-Newtonian region with the nearly constant viscosity; region Ⅲ corresponds to shear-thinning at high shear rates. However, not all TLCPs exhibit these three flow regions.

Figure 6 illustrates the relationship between the melt viscosity and shear rate of the TLCP at different shear temperatures. At low shear rates, the viscosity increases slightly with the increase in the shear rate. This is because the molecular chains of the cylindrical samples obtained by injection molding are highly oriented. At 280 ℃, the highly oriented cylindrical samples experience some entanglement at lower shear forces, leading to a slight increase in the viscosity. As the shear rate increases, the TLCP exhibits shear-thinning characteristics. The samples subjected to high shear forces also have highly oriented molecular chains. When the temperature rises to 285 ℃, even at lower shear forces, some entanglement occurs, leading to an increase in the viscosity. As the temperature increases, the viscosity of the TLCP exhibits a significant decrease, indicating a strong temperature dependence of the viscosity. At 280 ℃ and 285 ℃, the viscosity of the TLCP decreases by three orders of magnitude with the increasing shear rate, and as the temperature continues to rise, the decreasing trend of the viscosity becomes less pronounced. The increase in the viscosity at lower shear rates may be related to the liquid crystalline state of the polyester. Additionally, no distinct three flow regions are observed on the flow curve of the TLCP. Within a certain range of shear rates, it exhibits the characteristic of shear-thinning.

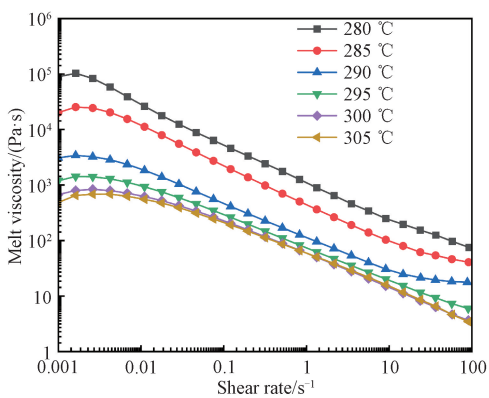

Fig. 6 Relationship between melt viscosity and shear rate of TLCP at different shear temperatures

Figures 7 – 9 illustrate the viscosity curves of the TLCP subjected to heat treatment at different shear temperatures for different times. The viscosity of the samples tends to decrease as the shear temperature increases. Additionally, at a constant temperature, the viscosity demonstrates the shear-thinning behavior with an increase in the shear rate. In the case of TLCPs, the rigid chains exhibit local orientation at low shear rates. However, with increasing of the shear rates, the rigid chains rapidly develop a broader range of orientations. Moreover, due to the strong intermolecular forces of the rigid chain structure, once orientation occurs, it is difficult to reverse. The extensive orientation range hinders the transfer of momentum between flow layers, leading to a significant reduction in the interlayer drag force and subsequently decreasing the melt viscosity.

Romo-Uribe et al.[37] reported that the dependence of the viscosity on the molecular mass for nematic copolyesters without flexible spacers could be represented as $\eta_0 \propto M^{4.1}$ (η_0 represents the zero shear viscosity, and M represents the viscosity-average molecular mass). This value (4.1) is distinctly different from the value of 3.4 for conventional polymer melts but lies within the range of values reported for nematic polymers with flexible spacers. The molecular mass of the TLCP correlates positively with the viscosity[38-39]. The viscosity curves of samples subjected to heat treatment at 240 ℃ for different times overlapped almost completely, indicating that there is no significant increase in the molecular mass after heat treatment at 240 ℃. However, the viscosity curves of samples subjected to heat treatment at 250 ℃ for different times start to disperse. At shear temperatures of 280, 285, 290 and 295 ℃, the viscosity of heat-treated samples is higher than that of untreated samples, suggesting an increase in the molecular mass of the TLCP due to heat treatment at 250 ℃. When the heat treatment temperature elevates to 260 ℃, the viscosity curves for different heat treatment times show greater dispersion, indicating a more pronounced increase in viscosity and a further improvement in the molecular mass of the TLCP. Additionally, the molecular mass of the samples subjected to heat treatment at 250 ℃ and 260 ℃ at a shear temperature of 280 ℃ increases with longer heat treatment time[40]. These results indicate that solid-phase condensation reactions are difficult at lower temperatures, while they are accelerated at higher temperatures, leading to a rapid increase in the molecular mass. Therefore, to obtain a higher molecular mass of the TLCP, a higher heat treatment temperature and longer treatment time should be selected.

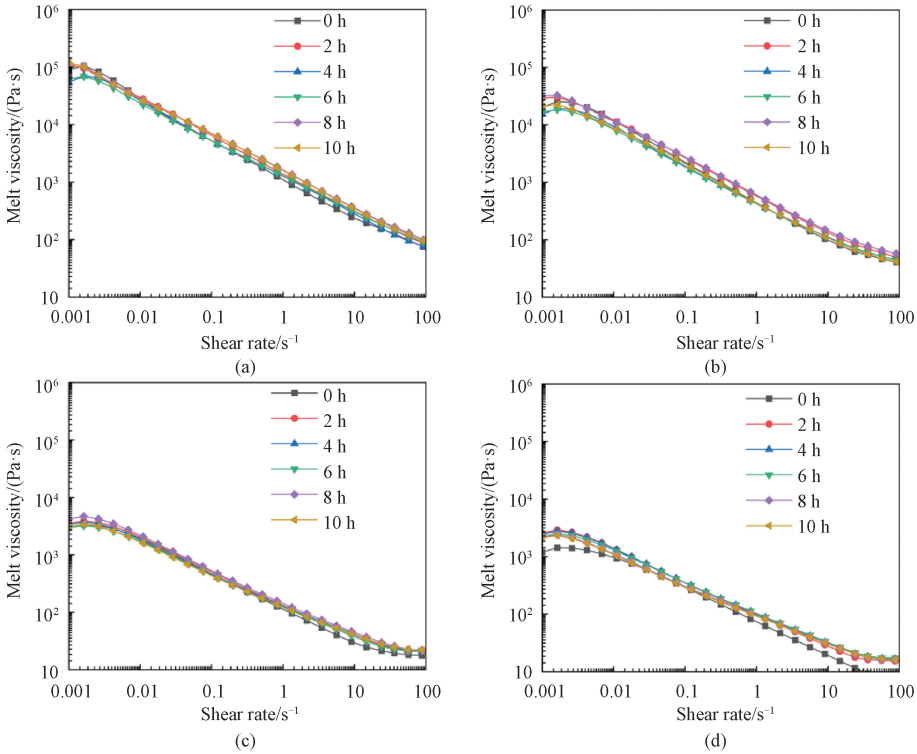

Fig. 7 Viscosity curves of TLCP after heat treatment at 240 ℃ for different times at specific shear temperature: (a) 280 ℃; (b) 285 ℃; (c) 290 ℃; (d) 295 ℃

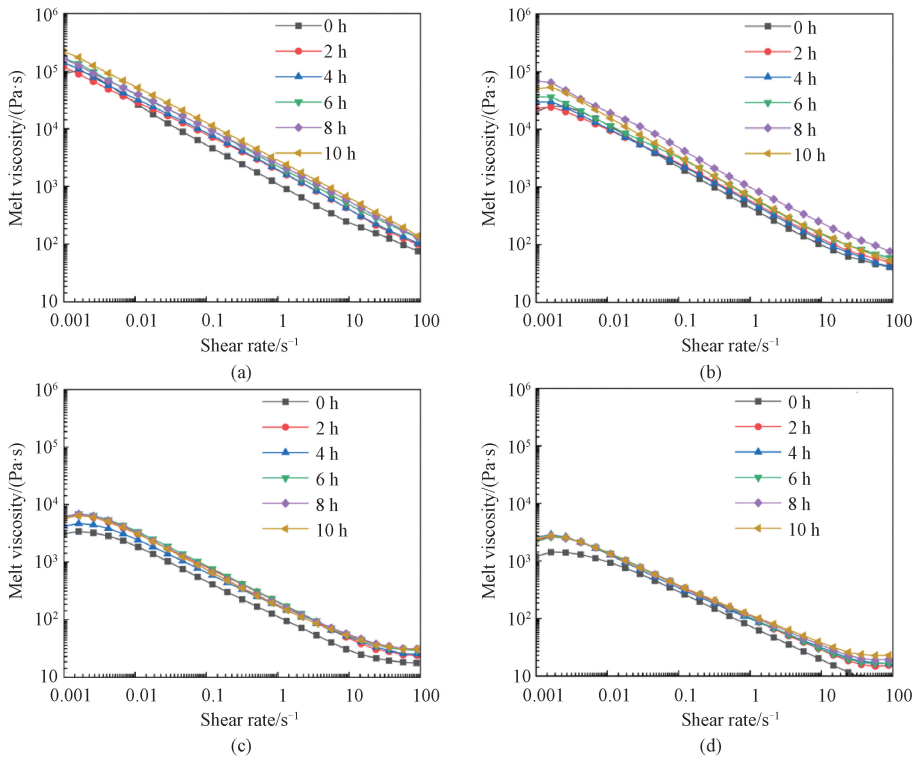

Fig. 8 Viscosity curves of TLCP after heat treatment at 250 ℃ for different times at specific shear temperature: (a) 280 ℃; (b) 285 ℃; (c) 290 ℃; (d) 295 ℃

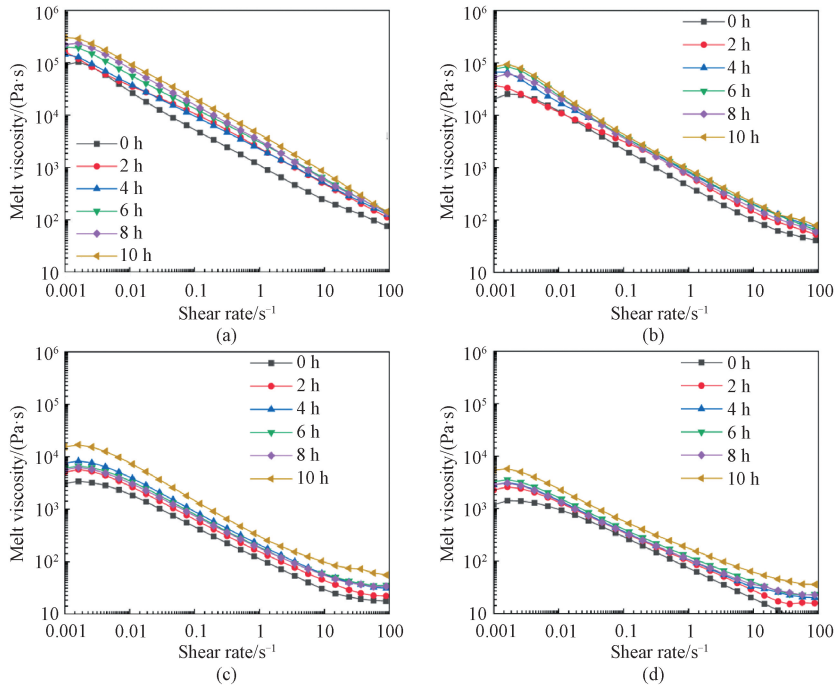

Fig. 9 Viscosity curves of TLCP after heat treatment at 260 ℃ for different times at specific shear temperature: (a) 280 ℃; (b) 285 ℃; (c) 290 ℃; (d) 295 ℃

3 Conclusions

A TLCP at a molar ratio of 7∶3 of HBA to HNA was prepared using a two-step melt polymerization method. The TLCP was subjected to solid-phase condensation by using a DSC. Experimental results showed that after eliminating the thermal history, heat treatment at 260 ℃ for 4 h improved the melting temperature of the TLCP from 260.9 ℃ to 264.6 ℃. However, further extending the heat treatment time resulted in a decrease in the melting temperature. The slower diffusion of small molecules due to the adhesive linkage of granular samples leads to an increase in by-products within the granular samples, resulting in a lower melting temperature. After heat treatment at 250 ℃, the glass transition temperature rose from 108.0 ℃ to 111.6 ℃. Observation of the viscosity curves of the TLCP revealed marked changes in the viscosity for different treatment times at 260 ℃. At higher temperatures, the reaction rate of solid-phase condensation was faster, leading to rapid growth in the molecular mass. In summary, heat treatment resulted in an enhancement of the melting temperature, glass transition temperature and molecular mass of the TLCP. However, the impact of heat treatment on TLCP is complex and requires a comprehensive consideration of treatment conditions.

References

[1] LYU X L, XIAO A Q, SHI D, et al. Liquid crystalline polymers: discovery, development, and the future [J]. *Polymer*, 2020, 202: 122740.

[2] SCHALLER R, PEIJS T, TERVOORT T A. High-performance liquid-crystalline polymer films for monolithic "composites" [J]. *Composites Part A: Applied Science and Manufacturing*, 2016, 81: 296-304.

[3] KOMATSU S, WETZEL B, FRIEDRICH K. Novel liquid crystal polymers with tailored chemical structure for high barrier, mechanical and tribological performance [M]. Cham: Springer, 2015: 15-39.

[4] RAMATHAL H, LAWAL A. Barrier properties of a thermotropic liquid-crystalline polymer[J]. *Journal of Applied Polymer Science*, 2003, 89(9): 2457-2463.

[5] WEINKAUF D H, PAUL D R. Gas transport properties of thermotropic liquid-crystalline copolyesters. I. The effects of orientation and annealing[J]. *Journal of Polymer Science Part B: Polymer Physics*, 1992, 30(8): 817-835.

[6] WEI P, LI L L, WANG L, et al. Synthesis and properties of high performance biobased liquid crystal copolyesters toward load-bearing bone repair application [J]. *European Polymer Journal*, 2022, 173: 111278.

[7] WANG S Y, MA S N, LI N, et al. Branched thermotropic liquid crystal polymer with favourable processability and dielectric properties [J]. *European Polymer Journal*, 2023, 196: 112302.

[8] THOMPSON D C, TANTOT O, JALLAGEAS

H, et al. Characterization of liquid crystal polymer (LCP) material and transmission lines on LCP substrates from 30 to 110 GHz[J]. *IEEE Transactions on Microwave Theory and Techniques*, 2004, 52(4): 1343-1352.

[9] GUAN Q B, LU X, CHEN Y Y, et al. High-performance liquid crystalline polymer for intrinsic fire-resistant and flexible triboelectric nanogenerators[J]. *Advanced Materials*, 2022, 34(34): e2204543.

[10] PARK G T, CHANG J H, LIM A R. Thermotropic liquid crystalline polymers with various alkoxy side groups: thermal properties and molecular dynamics[J]. *Polymers*, 2019, 11(6): 992.

[11] CHOI E J, LEE S J, JEONG Y G. Effects of mesogenic cycloaliphatic units on the microstructure and properties of thermotropic liquid crystalline polyesters[J]. *ChemistrySelect*, 2023, 8(1): e202203131.

[12] SONG B S, LEE J Y, JANG S H, et al. Fiber formation and structural development of HBA/HNA thermotropic liquid crystalline polymer in high-speed melt spinning[J]. *Polymers*, 2021, 13(7): 1134.

[13] DONG D W, JIANG S C, NI Y S, et al. Syntheses and properties of thermotropic copolyesters of *p*-hydroxybenzoic acid [J]. *European Polymer Journal*, 2001, 37(3): 611-617.

[14] LI X G, ZHOU Z L, WU X G, et al. Structure and properties of liquid crystalline naphthalenediol copolyesters [J]. *Journal of Applied Polymer Science*, 1994, 51(11): 1913-1921.

[15] KRIGBAUM W R, HAKEMI H, KOTEK R. Nematogenic polymers having rigid chains. 1. Substituted poly(*p*-phenylene terephthalates) [J]. *Macromolecules*, 1985, 18(5): 965-973.

[16] WEI P, CAKMAK M, CHEN Y W, et al. Aromatic liquid crystalline copolyesters with low T_m and high T_g: synthesis, characterization, and properties [J]. *Journal of Applied Polymer Science*, 2014, 131(13): 40487.

[17] WEI P, CAKMAK M, CHEN Y W, et al. The influence of bisphenol AF unit on thermal behavior of thermotropic liquid crystal copolyesters [J]. *Thermochimica Acta*, 2014, 586: 45-51.

[18] LENZ R W. Synthesis and properties of thermotropic liquid crystal polymers with main chain mesogenic units [J]. *Polymer Journal*, 1985, 17(1): 105-115.

[19] WEI P, LOU H J, YAN J F, et al. Synthesis and properties of high performance aromatic thermotropic liquid crystal copolyesters based on naphthalene ring structure[J]. *Polymer*, 2022, 240: 124472.

[20] BALLAUFF M, SCHMIDT G F. Rigid rod polymers with flexible side chains. 2. Observation of a novel type of layered mesophase [J]. *Die Makromolekulare Chemie, Rapid Communications*, 1987, 8(2): 93-97.

[21] PAN Z Y, GAO S X, ZHAO Y F, et al. Processability-enhanced aromatic thermotropic liquid crystalline copolyesters via the introduction of the unsymmetrical units [J]. *Journal of Applied Polymer Science*, 2023, 140(13): e53659.

[22] WEI P, WANG L, WANG X H, et al. Nonisothermal and isothermal oxidative degradation behavior of thermotropic liquid crystal polyesters containing kinked bisphenol AF and bisphenol A units [J]. *High Performance Polymers*, 2014, 26(8): 935-945.

[23] JACKSON W J Jr. Liquid crystalline polymers. 5. Liquid crystalline polyesters containing naphthalene rings [J]. *Macromolecules*, 1983, 16(7): 1027-1033.

[24] LANGELAAN H C, DE BOER A P. Crystallization of thermotropic liquid crystalline HBA/HNA copolymers[J]. *Polymer*, 1996, 37(25): 5667-5680.

[25] PARK S, NA Y J, KIM A Y, et al. Annealing effect of thermotropic liquid crystalline copolyester fibers on thermo-mechanical properties and morphology [J]. *Scientific Reports*, 2022, 12: 13100.

[26] SARLIN J, TÖRMÄLÄ P. Heat treatment studies of a TLCP fiber[J]. *Journal of Applied Polymer Science*, 1993, 50(7): 1225-1231.

[27] SARLIN J, TÖRMÄLÄ P. Isothermal heat treatment of a thermotropic LCP fiber [J]. *Journal of Polymer Science Part B: Polymer Physics*, 1991, 29(4): 395-405.

[28] KIM Y C, ECONOMY J. The mechanical properties of thermally treated 73/27 HBA/HNA copolyester [J]. *Polymers for Advanced Technologies*, 1999, 10(8): 493-500.

[29] LEE W J, KWAC L K, KIM H G, et al. Thermotropic liquid crystalline copolyester fibers according to various heat treatment conditions [J]. *Scientific Reports*, 2021, 11: 11654.

[30] REYES-MAYER A, ROMO-URIBE A, JAFFE M. Structure evolution of thermotropic polymers by thermal annealing. A light and X-ray scattering study [J]. *MRS Online Proceedings Library*, 2015, 1765(1): 65-70.

[31] SCHNEGGENBURGER L A, OSENAR P, ECONOMY J. Direct evidence for sequence ordering of random semicrystalline copolyesters during high-temperature annealing [J]. *Macromolecules*, 1997, 30(13): 3754-3758.

[32] KAITO A, KYOTANI M, NAKAYAMA K. Effects of draw-down ratio and annealing

treatment on structure formation in extruded strands of a thermotropic liquid crystalline copolyester [J]. *Journal of Macromolecular Science, Part B*, 1995, 34(1/2): 105-118.
[33] ROMO-URIBE A, REYES-MAYER A, SARMIENTO-BUSTOS E, et al. Synchrotron scattering and nanoindentation of heat treated high performance thermotropic polymer [J]. *MRS Advances*, 2018, 3(62): 3709-3714.
[34] KIM Y C, ECONOMY J. The degradation process observed during step annealing of 73/27 HBA/HNA copolyester [J]. *Macromolecules*, 1999, 32(9): 2855-2860.
[35] ROMO-URIBE A, REYES-MAYER A, CALIXTO RODRIGUEZ M, et al. On the influence of thermal annealing on molecular relaxations and structure in thermotropic liquid crystalline polymer [J]. *Polymer*, 2022, 240: 124506.
[36] REYES-MAYER A, ALVARADO-TENORIO B, ROMO-URIBE A, et al. SALS, WAXS and mechanical properties of heat-treated thermotropic polymers [J]. *Polymers for Advanced Technologies*, 2013, 24(12): 1029-1039.
[37] ROMO-URIBE A, WINDLE A H. Melt viscosity of main-chain thermotropic liquid crystalline polymers without flexible spacers [J]. *Macromolecules*, 1995, 28(21): 7085-7087.
[38] HEBERER D P, ODELL J A, PERCEC V. Rheology and flow-induced liquid crystal phase transitions in thermotropic polyethers [J]. *Journal of Materials Science*, 1994, 29(13): 3477-3483.
[39] KAITO A, KYOTANI M, NAKAYAMA K. Effects of annealing on the structure formation in a thermotropic liquid crystalline copolyester [J]. *Macromolecules*, 1990, 23(4): 1035-1040.
[40] WARNER S B, LEE J. Towards understanding the increase in strength of thermotropic polyesters with heat treatment [J]. *Journal of Polymer Science Part B: Polymer Physics*, 1994, 32(10): 1759-1769.

热处理工艺对热致液晶聚芳酯分子量及热性能的影响

董世航[1], 陈宇锋[1], 万 海[1], 梁 源[2], 黄铄涵[1], 王燕萍[1], 夏于旻[1*]
1. 东华大学 高性能纤维及制品教育部重点实验室, 材料科学与工程学院, 上海 201620
2. 东华大学 物理学院, 上海 201620

摘 要: 热致液晶聚芳酯(thermotropic liquid crystal polyester, TLCP)纤维是一种重要的战略性高性能纤维。该文以4-羟基苯甲酸(HBA)和6-羟基-2-萘甲酸(HNA)作为共聚单体(摩尔比为7∶3), 通过两步熔融缩聚法制备了TLCP。通过傅里叶变换红外光谱和核磁共振波谱确认了TLCP的结构。利用差示扫描量热仪、动态热机械分析仪和高温旋转流变仪分析了热处理前后TLCP的热性能和流变学特性。结果表明, 经过热处理后, TLCP的熔点、玻璃化转变温度和熔体黏度显著增加, 这表明TLCP的结晶更加完善, 并且在热处理过程中发生了固相缩聚反应, 增加了其分子量。总之, 在低于但接近熔点的温度条件下进行热处理可以有效调节TLCP的结构和性能, 该研究结果可为TLCP纤维的高强化提供参考。

关键词: 热致液晶聚芳酯; 热处理; 黏度; 热性能